WATER RESOURCES RESEARCH, VOL. 20, NO. 10, PAGES 1390–1400, OCTOBER 1984

A Model for Investigating Mechanical Transport in Fracture Networks

H. K. ENDO AND J. C. S. LONG

Earth Science Division, Lawrence Berkeley Laboratory, University of California, Berkeley

C. R. WILSON

Hydrotechnique Associates, Berkeley, California

P. A. WITHERSPOON

Earth Science Division, Lawrence Berkeley Laboratory, University of California, Berkeley

A technique is presented to determine when anisotropic fracture systems can be modeled as equivalent porous media (continua) for transport. In order to use the continuum approach, one must demonstrate that the fracture system has the same transport behavior as an equivalent porous medium. Hydraulic effective porosity is calculated as the product of specific discharge and mean travel time, divided by linear length of travel. Specific discharge and hydraulic effective porosity are measured in different directions of flow in regions of varying size with constant hydraulic gradients. If the fracture system behaves like an equivalent porous medium, directional flow has the following properties: (1) specific discharge can be predicted from a permeability tensor and (2) hydraulic effective porosity is independent of direction of flow. A numerical model has been developed to simulate mechanical transport under steady flow in a discrete fracture network. The model is used to determine the distribution of travel times from inlet to outlet for fluid traveling in stream tubes. We have examined only systems with parallel fracture sets in which all fractures are long compared to the region under study. These systems satisfy criterion 1 in that flux can be calculated using a porous medium equivalent. However, these systems do not satisfy criterion 2 because hydraulic effective porosity is shown to be directionally dependent. Thus, even though flux can be accurately predicted using porous medium assumptions for some fracture systems, it may not be possible to accurately predict mechanical transport using these same assumptions.

INTRODUCTION

Concerns about radioactive waste storage and the injection of toxic pollutants deep underground have focused interest on the problems of fluid flow and mass transport in groundwater systems. The disposal of pollutants in or near a rock mass where fractures constitute the major conduits of groundwater movement is a central problem. This paper presents a technique for determining when fracture networks can be modeled as equivalent porous media in transport studies. When the porous medium approach is not appropriate, a discrete model that simulates transport in each fracture of the network must be used. However, the discrete approach requires detailed information on the geometry of the fracture system and thus may require an excessive amount of data and computational effort. The advantage of the continuum approach is that average properties are analyzed such that the detailed fracture geometry and simulation of transport within each fracture are not required. Thus the continuum approach is preferable if it can be shown to be appropriate.

In order to evaluate whether the continuum approach is applicable, one must be able to demonstrate that the fracture system has the same transport behavior as that of an equivalent porous medium. However, the fracture system may be anisotropic and transport in anisotropic media is not fully understood. The reason for this is that no solution is available to determine the components of the dispersivity tensor in an anisotropic medium [*Freeze and Cherry*, 1979, p. 552].

Paper number 4W0816.

However, mechanical transport, the component of transport that is simply due to the movement of fluids along the flow paths, can be evaluated for anisotropic media. Thus, if we restrict our attention to mechanical transport, we can investigate the conditions under which fractured rock masses behave hydraulically like porous media. In the literature, mechanical transport is often referred to as advective transport.

To understand mechanical transport, we need to be able to evaluate the ratio of fluid flux to mean velocity, tortuosity, and mechanical dispersion, all as a function of direction of flow. In an anisotropic porous medium, the ratio of flux to mean velocity is assumed to be independent of direction of flow and equal to the porosity. Thus a test for equivalent porous medium behavior is to determine if the ratio of flux to velocity is constant in all directions. Less is understood about the directional dependence of tortuosity and mechanical dispersion in anisotropic porous media. Thus evaluation of these parameters in anisotropic fracture networks may teach us something about transport in all permeable media.

A numerical model is used in this research to simulate mechanical transport in discrete fracture networks. We assumed that mechanical transport is the only transport process and that the fluid flow is restricted to planar fractures within an impermeable rock matrix. The model developed in this work is used to simulate mechanical transport by tracing fluid movement within streamtubes that interconnect the inflow and outflow boundaries of a fracture system.

It should be emphasized that this simulation of transport is only useful for determining whether or not the system behaves as a porous medium. The analysis does not reveal how a tracer that is subject to diffusion and chemical reactions will migrate through the network.

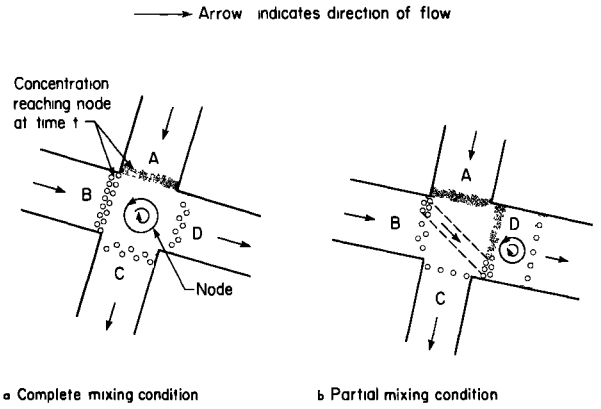

Fig. 1. Graphical representation at a node of (*a*) complete mixing and (*b*) partial mixing.

REVIEW OF LITERATURE

The hydraulic effective porosity is used in this work to express the relationship between flux and mean velocity, and is defined as the ratio of specific discharge to average linear velocity. The average linear velocity is the straight or linear travel length divided by the mean flow travel time. Laboratory and field studies have demonstrated that for isotropic porous media the hydraulic effective porosity ϕ_H is not necessarily equal to the total porosity ϕ [*Von Rosenburg*, 1956; *Biggar and Nielsen*, 1960; *Hazzaa et al.*, 1965, 1966; *Grove and Beetem*, 1971; *Hoehn and Roberts*, 1982]. Experimental evidence from the laboratory indicates that the relationship between ϕ_H and ϕ is dependent on the type of porous medium. Where there is a well-ordered pore structure (i.e., glass beads), ϕ_H is approximately equal to ϕ. However, where the pore structure is irregular and nonuniform, the hydraulic effective porosity differs from the total porosity and is usually less than ϕ because of the presence of stagnant void regions.

A numerical model can be used to simulate a tracer experiment to evaluate ϕ_H when the properties of the porous medium are known. The porous medium is divided into small interconnected subregions called elements, and transport is modeled within each element. For a fractured rock mass the equivalent element would be a segment of a fracture. Elements are interconnected to one another at fracture intersections called nodes.

Such discrete numerical models have been used by several workers to simulate transport in a network of fractures. In a series of four related papers [*Castillo et al.*, 1972; *Krizek et al.*, 1972; *Karadi et al.*, 1972] a numerical model was developed to simulate transport in a fracture system consisting of two sets of parallel, planar, and continuous fractures of constant aperture and spacing. The principles incorporated in this model can be understood by following the migration of solute as it flows through the fracture system. Mechanical transport governs the movement of solute within an element:

$$\frac{\partial c}{\partial t} + u(\eta)\frac{\partial c}{\partial \xi} = 0$$

When solute leaves an element at a node, it may encounter solute flowing into the node from other elements. Krizek et al. assumed that all inflowing solute was either completely or partially mixed at fracture intersections. In the complete mixing condition, all outflow elements receive the same concentration, given by

$$c_0(t) = \left[\sum_i \int_0^{b_i} u_i(\eta)c_i(\eta, t)\, d\eta\right](Q_N)^{-1}$$

where the summation of i is for all inflow elements. The complete mixing condition is illustrated in Figure 1*a*.

The partial mixing condition of Krizek et al. is illustrated in Figure 1*b*. Fluid enters the node from elements A and B and exits through elements C and D. Element D is a large element such that the flow rate in element D consists of the total flow rate in element A and part of the flow rate in element B. The widths in elements A and B occupied by the flux flowing into element D are determined, and the mass of solute entering the node from these zones is calculated. This mass of solute is then distributed uniformly across the entrance to element D.

Schwartz et al. [1981] stochastically generated two orthogonal fracture sets in a rectangular domain. The number of fractures in each set within the domain was controlled by the areal density (the number of fractures per unit area). The fracture centers were randomly distributed in the domain, and the fracture lengths and apertures were generated from exponential and lognormal distributions, respectively. Schwartz et al. avoided a major simplification made in previous transport studies of fracture systems by using fractures of finite length. Impermeable boundaries were created on two opposing sides of the rectangular domain, and constant head boundary conditions were applied to the two remaining sides. Tracer particles were assumed to propagate at a constant velocity within the elements and were also assumed to be completely mixed at the nodes. Molecular diffusion was considered to be negligible within a fracture and thus was not modeled.

Schwartz et al. [1981] found that the spatial particle distribution in the average direction of flow was non-Gaussian and positively skewed. The skewness is attributed to a combination of channels of rapid movement oriented in the direction of flow and channels of slow movement oriented normal to the direction of flow. The bulk of the fluid moves in the direction of gradient, and the majority of the particles travel in this direction. However, as time proceeds, the probability of a particle flowing into a slow channel increases. As particles move through the slow channels, an asymmetrical particle distribution develops.

THE NUMERICAL MODEL

The numerical approach used in this study to investigate mechanical transport in a network of fractures simulates the

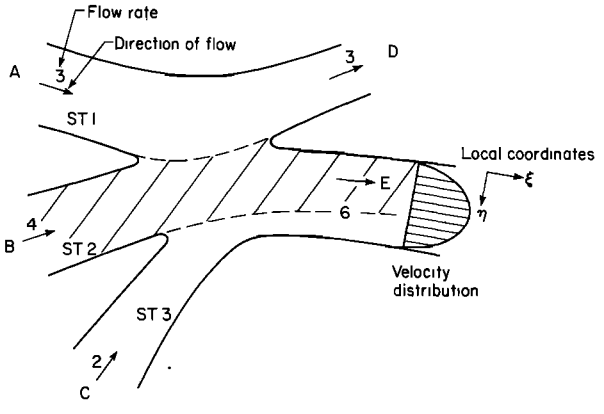

Fig. 2. Redistribution of stream tubes at a node.

detailed movement of fluid within streamtubes through the fracture network. This numerical model operates in three stages: (1) generation of the fracture system, (2) calculation of flow rates in each fracture and determination of macroscopic flow properties, and (3) simulation of mechanical transport in the fracture network and determination of macroscopic mechanical transport properties.

In the first stage a two-dimensional fracture system is created in an area called the generation region. The procedure used in creating the fracture system was developed by *Long et al.* [1982]. The fractures in the generation region are created one set at a time, and the number of fractures in each set is controlled by an assigned areal density. The geometric parameters required to create each fracture are: its length, orientation, aperture, and location in the generation region. This information may be read directly into the computer program (deterministic approach) or may be generated stochastically. In a stochastic generation, each fracture is randomly located in the generation region to create a statistically homogeneous system. The three remaining geometric parameters are each created by probabilistic simulation. Probabilistic simulation can be conducted with either the Gaussian, lognormal or exponential probability distribution. The mean and standard deviation for the simulated distribution must be read into the computer program.

A flow region within the generated fracture network is selected for mechanical transport studies. The flow region may be oriented in any direction as long as it fits within the boundaries of the generation region. A finite element mesh is generated for this flow region consisting of nodes, which are fracture intersections, and elements, which are fracture segments between nodes. This constitutes the first stage of the numerical model.

In the second stage the hydraulic head at each node and flow rate in each element are calculated using a finite element technique developed by *Wilson* [1970]. The cubic law for laminar flow governs the flow rate in each planar fracture. The appropriate boundary conditions that apply to the flow region in order to evaluate the hydraulic effective porosity will be discussed in the next section.

In the final stage, mechanical transport is simulated for the fractures in the flow region. In this work, a stream tube is defined as a flow conduit that is bounded by streamlines in which the flow rate is constant. The model developed to simulate mechanical transport is used to determine the paths and flow rates for the stream tubes in the fracture network. Once all the stream tube paths have been determined, the total travel time from the inlet to outlet for the fluid in each stream tube is computed by summing the residence times in each element along the individual stream tubes. This procedure requires an evaluation of the path, the flow rate, and the width

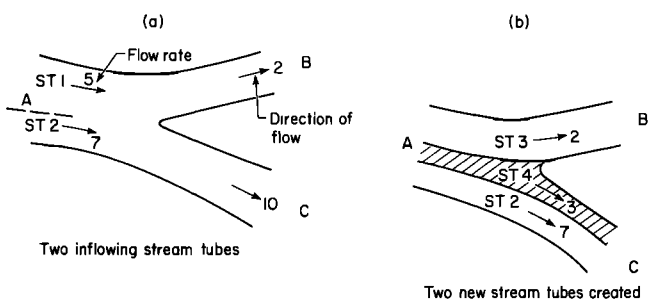

Fig. 3. Creation of new stream tubes at a node.

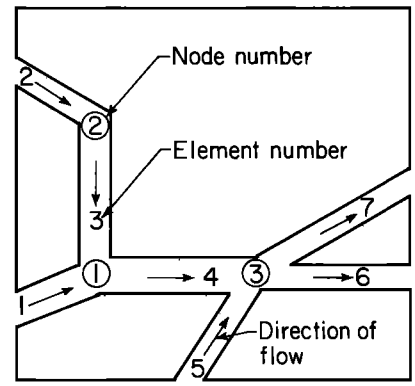

Fig. 4. Fracture network with inflow stream tubes initiated in elements 1, 2, and 5.

of the stream tube in each element. We will first consider the time it takes the fluid in a stream tube to travel the length of an element. Since fluid flows out of an element into a node, we will then discuss the way that stream tubes are traced through nodes.

As mentioned earlier, the flow rate in an element is governed by the cubic law for fracture flow. It can be shown that by solving the Navier-Stokes equation for laminar flow between parallel plates, an expression for the well-known parabolic velocity distribution across a planar element is obtained:

$$u(\eta) = \frac{\rho g}{\mu}\frac{d\Phi}{d\xi}\left[\frac{\eta^2}{2} - \frac{b}{2}\eta\right] \tag{1}$$

The flow rate in the element is obtained by integrating (1) across the width of the element:

$$Q_f = \int_0^b u(\eta)\, d\eta = -\frac{\rho g b^3}{12\mu}\frac{d\Phi}{d\xi}$$

This is the cubic law for fracture flow.

The time it takes the fluid in a stream tube to travel the length of an element is given by

$$t_{ST} = L_T\left(\frac{Q_{ST}}{\eta_{i+1} - \eta_i}\right)^{-1}$$

where η_{i+1} and η_i are the bottom and top coordinates, respectively, defining the width of the stream tube within the element. Thus, to determine t_{ST}, the width of the stream tube must be computed. Integrating (1) between η_i and η_{i+1} yields

$$Q_{ST} = \int_{\eta_i}^{\eta_{i+1}} u(\eta)\, d\eta = \frac{6Q_f}{b^3}\left[\frac{b(\eta_{i+1}{}^2 - \eta_i{}^2)}{2} - \frac{(\eta_{i+1}{}^3 - \eta_i{}^3)}{3}\right] \tag{2}$$

The width occupied by the stream tube can then be determined knowing the flow rate in the stream tube and the top coordinate η_i. For example, the node in Figure 2 consists of three inflowing stream tubes labeled ST1, ST2, and ST3. Stream tube ST2 has a flow rate of 4 units and a top coordinate $\eta_{i,2}$ equal to zero in element E. The bottom coordinate of ST2, $\eta_{i+1,2}$, is obtained using (2). That coordinate then becomes the top coordinate for ST3 in element E, from which the travel time for ST3 in element E is determined.

The principle of conservation of mass and the physics of laminar flow are used to calculate the downstream location of inflow stream tubes in outflow elements at a node. Travel

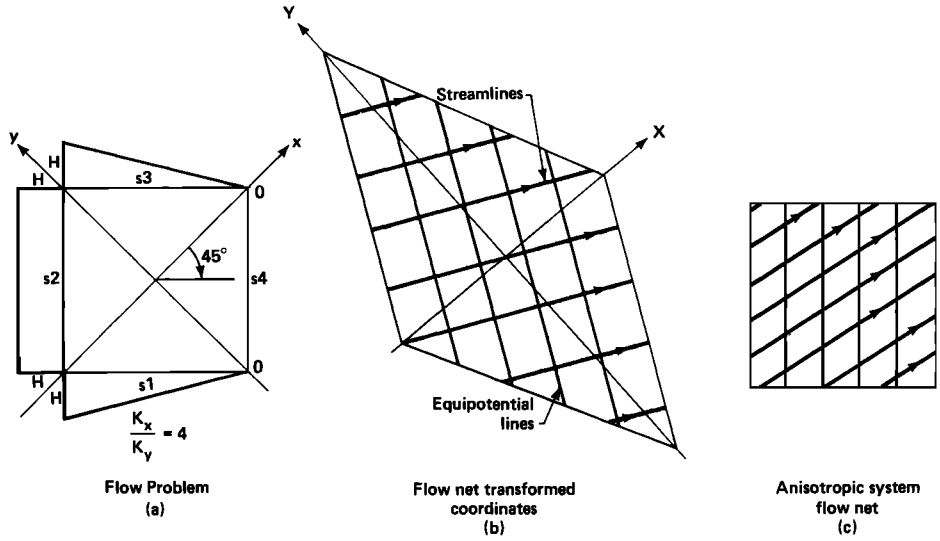

Fig. 5. Flow field for an anisotropic porous medium with a constant hydraulic gradient.

times within a node are considered to be negligible. The upper outflow element D in Figure 2 has a flow rate of 3 units. The flow into this element must come from ST1 because if any of the other two stream tubes flowed into element D, they would have to cross the path of ST1. In laminar flow the fluid flows in layers, one layer flowing smoothly over the adjacent layers. Using the same principle, ST2 must occupy the upper and ST3 the lower portion of element E. The order of the stream tubes and the flow rate in each stream tube are recorded for each outflow element. This information is needed to determine the travel time for the fluid in each stream tube. Thus no mixing is assumed to occur at fracture intersections.

Laboratory experiments performed by *Krizek et al.* [1972] led to the conclusion that the complete mixing condition at intersections is valid for laminar flow. However, these experiments were not conclusive. They were limited to the situation in which there was only one inflow element and all outflow elements had nearly identical flow rates. A more general set of experiments should be considered which involves more than one inflow element, with unequal flow rates and unequal concentrations in both inflow and outflow elements. *Wilson* [1970] conducted such an experiment using capillary tubes for Reynolds numbers on the same order as the experiments of *Krizek et al.* [1972]. Wilson demonstrated that fluid flows within layers at intersections when the flow is laminar.

The flux in an inflow stream tube can be distributed into more than one outflow element at a node, as illustrated for ST1 in Figure 3. When this arises, the inflow stream tube must be subdivided such that a new stream tube is created for every outflow element that receives any portion of the inflow. For example, ST3 and ST4 are the result of the subdivision of the discontinued stream tube ST1. The total travel time to this particular node for the fluid in a new stream tube is determined by backtracking along the path of ST1 to its origin.

The general procedure used in tracing the location of stream tubes in the fracture network begins by assigning a stream tube to every inflow element on the boundary of the flow region. This assures that stream tubes exist in every conductive element within the flow region. For example, in the fracture network shown in Figure 4, stream tubes have been initiated in elements 1, 2, and 5. Each assigned stream tube is given a width equal to the aperture of the element it occupies and a flow rate equal to that in the element.

The program then proceeds in sequential nodal order determining the outflow stream tubes at each node. The outflow stream tubes at a node can only be determined if the stream tubes are known in all inflow elements at the node. If stream tubes have not yet been calculated for an inflow element, the inflow element number and the node number are temporarily stored in memory. This situation arises when an inflow element at the node under consideration is an outflow element at a higher numbered node. The stream tubes in the inflow element at the current node can only be determined after proceeding to the higher node. In Figure 4, node 1 is the first node examined by the computer program, and element 4 is the only outflow element at this node. The stream tubes in element 4 can only be calculated if the stream tubes are known in inflow elements 1 and 3. The stream tube in element 1 is known, since a stream tube was assigned to this element in the first phase of the stream tubing procedure. However, at this point, the stream tubes in element 3 are unknown. Therefore element 3 and node 1 are stored in memory, and the program proceeds to node 2.

The stream tubes in the outflow elements at a node are determined when the stream tubes have been calculated for all inflow elements. After the stream tubes in all outflow elements have been determined, the program scans the elements stored in memory to remove any element that is an outflow element at the current node, because the stream tubes are known in these elements. If an element is the only one stored for a particular node, then all the outflow stream tubes at that node are determined. For example, at node 2 for the fracture network in Figure 4 the stream tube for the inflow element 2 is known. The stream tube in the outflow element 3 can therefore be computed knowing the stream tube in element 2. The program then removes element 3 from the list of stored elements because the stream tube in element 3 has been determined. Inasmuch as element 3 is the only element stored in memory for node 1, the stream tubes in the outflowing element 4 at node 1 can now be calculated. As the network is

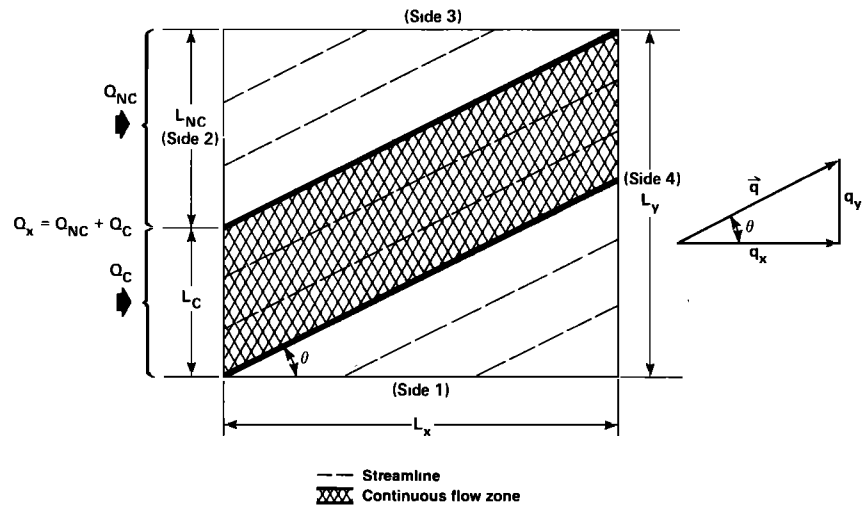

Fig. 6. Example of groundwater flow in an anisotropic porous medium, showing a cross-hatched zone where travel length is constant.

scanned in this fashion, the number of stream tubes increases and the width of stream tubes decreases because of the creation of new stream tubes at nodes.

Hydraulic Boundary Conditions for Determining Hydraulic Effective Porosity

One important use of this model is to measure hydraulic effective porosity (ϕ_H) to determine the degree of porous media equivalence for fracture networks. For an equivalent porous medium, hydraulic effective porosity is equal to the product of q and the mean flow travel time, divided by the linear length of travel. If it can be shown that the specific discharge and the linear travel length are constant, then the mean travel time is the only parameter that must be measured to evaluate hydraulic effective porosity. The specific discharge criterion will be satisfied if the flow system is shown to behave as an equivalent porous medium for fluid flux when the proper hydraulic boundary conditions are applied to the fracture system. The linear travel length criterion will be satisfied by an appropriate selection of a test section within the fracture system.

To establish this desired flow system, the model has been designed to maintain certain hydraulic boundary conditions on the flow region. Figure 5 illustrates these boundary conditions, which are designed to create a uniform specific discharge if the medium behaves as an anisotropic, homogeneous continuum. First, as shown in Figure 5*a*, constant hydraulic heads of H and 0, respectively, are fixed on sides 2 and 4 of the flow region. Then constant hydraulic gradients are maintained along sides 1 and 3. A constant hydraulic gradient in the flow field is needed to assure that $\mathbf{q}$ will be uniform throughout the flow region in accordance with Darcy's law. The uniform flow field (Figure 5*c*) for this anisotropic medium can be determined using flow net theory. Figure 5*b* shows the flow net in the transformed isotropic space [*Freeze and Cherry*, 1979, pp. 174–178]. If no-flow boundary conditions had been applied along sides 1 and 3, a nonuniform flow field would have developed in the flow region unless the direction of the hydraulic gradient coincided with a direction of principal permeability.

The remaining condition is for the linear length of travel to be constant within the region where mechanical transport is measured. This condition is maintained within the cross-hatched zone in Figure 6 where fluid flows continuously between sides 2 and 4. Thus, once the boundary conditions have been established, as illustrated in Figure 5*a*, a test section is defined where specific discharge and linear travel length will be constant for fracture systems behaving as equivalent porous media for fluid flux, and the hydraulic effective porosity can be determined simply by measuring the mean travel time within this test section.

Equivalent Porous Medium Behavior

The primary objective of this study is develop a method to determine whether a given fracture system can be treated as an equivalent homogeneous porous medium continuum. The requirements for continuum flow behavior are presented in this section, followed by a discussion of continuum behavior for transport.

In a porous medium, Darcy's law makes it possible to evaluate macroscopic fluid flux properties by treating the medium as an equivalent continuum. Fluid flow characteristics can be analyzed for equivalent porous medium behavior in two ways. First, flow fields created from the boundary conditions shown in Figure 5 are individually evaluated for equivalent porous medium behavior. Then, directional flow is analyzed by synthesizing flow results in different directions [*Long et al.*, 1982]. In a porous medium, directional flow characteristics can be predicted from a unique permeability tensor.

Each flow field must satisfy the following two requirements in order to exhibit equivalent homogeneous porous medium behavior:

1. The macroscopic flow field can be predicted by Darcy's law.
2. The specific discharge is stable and does not fluctuate with the size of the flow region.

Under the boundary conditions presented earlier, the flow field for an anisotropic porous medium is characterized by a uniform specific discharge. Because the specific discharge is a vector, the condition of uniformity implies that both its magnitude and angle of flow are constant. The use of macroscopic flow measurements are described below to determine if the magnitude and angle of $\mathbf{q}$ are constant for a given flow field.

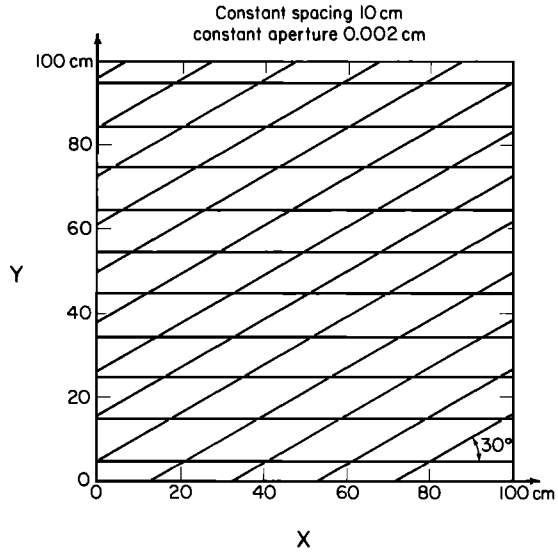

Fig. 7. Fracture system with two sets of parallel, continuous, and constant aperture fractures.

A uniform specific discharge means that parallel cross sections of equal area will have the same total fluid flux flowing across them. This means that in Figure 6 the flow rate into side 2 is equal to the flow rate out of side 4:

$$Q_{S2} = Q_{S4} \tag{3}$$

and the flow rate into side 1 is equal to the flow rate out of side 3:

$$Q_{S1} = Q_{S3} \tag{4}$$

Equations (3) and (4) constitute a continuity test to evaluate if the magnitude of the specific discharge is constant.

Two approaches are used to determine the angle of flow. Both approaches produce the same angle of flow if the specific discharge is uniform. In the first approach the flow rates into the sides of the flow region are used to compute the components of the specific discharge in the direction of the hydraulic gradient and in the direction perpendicular to the hydraulic gradient. The angle of flow is then calculated from these results. This calculation is not based on the path of the fluid. In the second approach the conditions of the uniform flow field are used to compute angle of flow. As shown in Figure 6, the amount of fluid entering side 2 that exits on side 4 can be used to compute angle of flow. The remaining fluid entering side 2 must exit on side 3.

The first method of determining the angle of flow can be expressed mathematically using the two components of the specific discharge:

$$\mathbf{q} = q_x\hat{i} + q_y\hat{j}$$

or, referring to Figure 6,

$$\theta = \tan^{-1}\frac{q_y}{q_x} = \text{ANFD} \tag{5}$$

For the flow region in Figure 6 the specific discharge in the x direction is obtained by summing the flow rate into side 2 from the individual flow channels and dividing by L_y. Similarly, the total flow rate into side 1 divided by L_x determines q_y.

The second method of determining the angle of flow is based on the uniformity of the specific discharge. For the anisotropic medium in Figure 6 a certain amount of flux entering side 2, Q_{NC}, must exit on side 3. Thus,

$$Q_{NC} = Q_{S3}$$

$$q_y = \frac{Q_{S3}}{L_x} = \frac{Q_{NC}}{L_x}$$

Substituting q_y into (5) yields

$$\theta = \tan^{-1}\frac{Q_{NC}}{q_x L_x} = \text{ANFC} \tag{6}$$

This relationship can also be obtained directly from the uniformity of the flow field. The cross-hatched area in Figure 6 designates the zone in which the fluid flows continuously from sides 2 to 4. Since the specific discharge is uniform, the following relationships hold on side 2:

$$\frac{Q_C}{L_C} = \frac{Q_{NC}}{L_{NC}} = \frac{Q_x}{L_y}$$

which means

$$L_{NC} = \frac{Q_{NC}L_C}{Q_C} = \frac{Q_{NC}L_y}{Q_x} = \frac{Q_{NC}}{q_x}$$

The relationship for the angle of flow is

$$\tan\theta = \frac{L_{NC}}{L_x} = \frac{Q_{NC}}{L_x q_x}$$

so

$$\theta = \tan^{-1}\frac{Q_{NC}}{q_x L_x} \tag{7}$$

which is the same expression as (6).

Equation (6) is the second method of computing the angle of flow. The evaluation of ANFD and ANFC constitutes the angle of flow test. The direction of the specific discharge is a constant if ANFD is equal to ANFC.

The stability of the specific discharge, the second requirement for a flow field to exhibit porous medium behavior for a particular direction of flow, is tested by slowly increasing the size of the flow region and measuring the specific discharge. Initially, the specific discharge may be expected to fluctuate significantly. In small flow regions the number of fractures may be too small so that the region cannot be treated like a representative elementary volume of a porous medium. However, as the side of the flow region increases, the fluctuations in

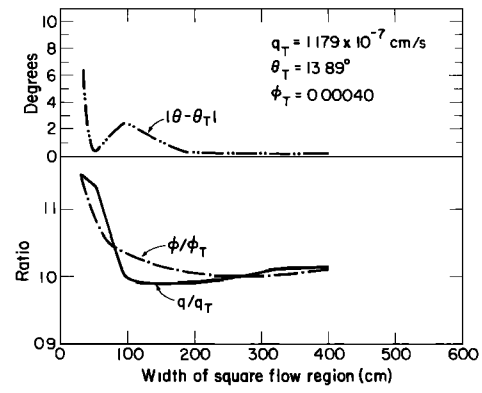

Fig. 8. Convergence of specific discharge and porosity to their theoretical values as size of flow region increases (ratio is q/q_T or ϕ/ϕ_T)

the specific discharge may dampen out, and eventually a stable value may be reached. When the specific discharge is stable, the system behaves like an equivalent porous medium for fluid flux.

The above tests can be used to examine equivalent porous medium behavior for a particular direction of flow. However, Darcy's law also specifies that the flow field in any direction can be predicted by a permeability tensor. If such a tensor exists, the square root of permeability in the direction of flow plots as an ellipse. Thus the shape of the plot of the square root of permeability is the test of whether directional flow for the system behaves like an equivalent porous medium.

To determine equivalent porous medium behavior for transport, one must examine the directional nature of the hydraulic effective porosity. The hydraulic effective porosity is traditionally assumed to be equal either to the total porosity or to the porosity calculated by considering only the conductive void regions. Since both porosities are independent of direction in an equivalent continuum, the hydraulic effective porosity should be constant in all directions. Thus the test for equivalent porous medium behavior for transport is to examine the stability of ϕ_H with direction.

Investigation of Continuous Fracture Systems

To demonstrate the use of the numerical model, the relationships between hydraulic effective porosity and total porosity were examined for two continuous systems of infinitely long fractures. Continuous systems were studied for two primary reasons. First, continuous fracture systems can be treated like equivalent porous media for fluid flux. *Snow* [1969] developed the equivalent porous media equations for q and θ for continuous fracture systems. The study of fracture systems with known continuum flow behavior can serve to demonstrate the tests developed to identify such behavior. Second, the possible directional dependence of the hydraulic effective porosity can be investigated for anisotropic fracture systems in which the void region is totally connected where there are no dead end zones.

System With Two Sets of Constant Aperture Fractures

In the first investigation of networks with continuous fractures the system consisted of two sets of parallel fractures oriented at 0° and 30°, as illustrated in Figure 7. All fractures had an aperture of 0.002 cm, and the spacing between fractures was a constant value of 10 cm.

Several different-sized flow regions were analyzed to investigate the requirement that a fracture system that exhibits porous medium behavior should have a specific discharge that remains stable. This study was conducted by varing the size of several square flow regions oriented at 0° and observing if the numerical solutions for q and θ converge to their theoretical values as size increases. The theoretical solutions for q and θ apply to flow regions of infinite dimensions. However, only finite-sized flow regions can be created using numerical models. Thus the difference between the theoretical and numerical solutions for q and θ should decrease as size increases.

TABLE 1. Specific Discharge Results for Fracture System With Two Sets of Parallel, Continuous, and Constant Aperture Fractures

Orientation of Gradient, degrees	Specific Discharge, 10^{-7} cm/s		Angle of Flow, degrees		
	Theoretical	Numerical	Theoretical	ANFC	ANFD
0	1.179	1.199	13.90	13.65	13.65
15	1.220	1.232	0	−1.47	0
30	1.179	1.184	−13.90	−13.84	−13.84
45	1.057	1.065	−27.63	−26.86	−26.86
60	0.8649	0.8706	−40.92	−40.82	−40.82
75	0.6147	0.6116	−52.91	−52.76	−52.76
90	0.3269	0.3406	−60.00	−61.32	−61.32
105	0.08759	0.0846	0	−2.87	−2.87

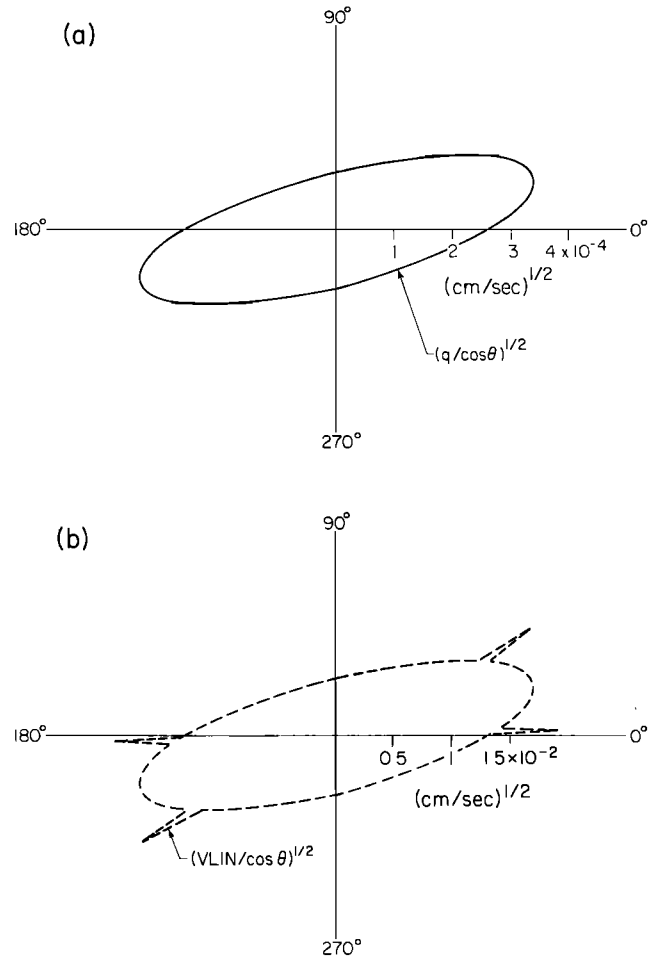

Fig. 9. Polar plots of (*a*) specific discharge and (*b*) average linear velocity factors versus direction of flow for system with two sets of parallel, continuous, and constant aperture fractures.

Figure 8 shows how the ratio of numerical to theoretical specific discharge (q/q_T) approaches unity as size of the flow region increases. The approach to porous medium equivalence is also evident from the results for angle of flow. As show on Figure 8, the deviation between the numerical and theoretical angles of flow ($|\theta-\theta_T|$) is negligible for flow regions larger than 200 × 200 cm. Further evidence that this size fracture network exhibits porous medium behavior can be obtained from the ratio of numerical to theoretical porosity (ϕ/ϕ_T), which has also been plotted on Figure 8. Thus the stability requirement is met for this particular fracture network when the size of the flow region is 200 × 200 cm or larger.

Next, flow results for different directions of flow were analyzed for equivalent porous medium behavior using the continuity and angle of flow tests. Flow regions oriented at every 15°, beginning at orientation 0°, were used in this part of the study. Square flow regions of width 400 cm were used for

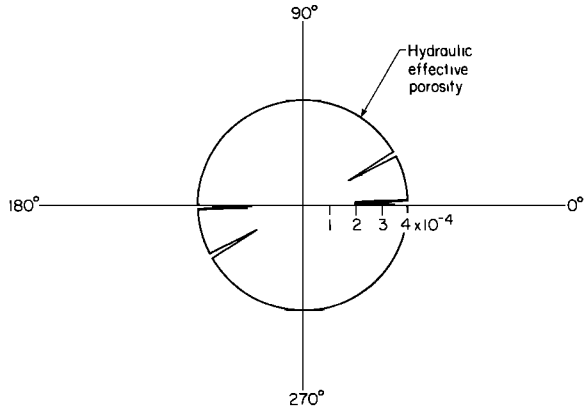

Fig. 10. Polar plot of hydraulic effective porosity versus direction of flow for system with two sets of parallel, continuous, and constant aperture fractures.

orientations 0°, 15°, 30°, 45°, 60°, and 105°. Rectangular flow regions 186 × 400 cm in size were used for orientations 75° and 90° because the angle of flow is greater than 45° for these two orientations. Side 2 had to be longer than side 1 to insure that a zone of continuous flow existed from side 2 to side 4.

A comparison of numerical and theoretical values for q and θ is given in Table 1. The flow results in Table 1 of $0.96 < q/q_T < 1.04$ and $|\theta - \theta_T| < 3°$ indicate that the stability requirement for porous medium behavior is satisfied for all flow regions regardless of the orientation of the flow field. The angle of flow test is also satisfied for all orientations because the values computed for ANFC are essentially identical to those of ANFD. Furthermore, the continuity test is also satisfied because flow rates on opposing sides of the flow region are equal. This equivalence results from the fact that an equal number of fractures from each set intersects opposing sides of each flow region. Thus each flow region that has been tested exhibits porous medium flow behavior.

Directional equivalent porous medium flow behavior can also be shown using the flow results in Table 1. *Marcus and Evenson* [1961] have derived very useful relationships between specific discharge and direction of flow for porous media. If the hydraulic gradient is kept constant, as was done in this study, the square root of the specific discharge divided by cos θ, $(q/\cos\theta)^{1/2}$, when plotted versus flow direction forms an ellipse for an equivalent porous medium, since $q/\cos\theta$ is equal to the product of the permeability in the direction of flow and the hydraulic gradient. Figure 9*a* shows the plot of $(q/\cos\theta)^{1/2}$ versus direction of flow. It may be seen that the specific discharge curve is an ellipse with directions of maximum and minimum permeabilities near 15° and 105°, respectively. The ellipse is symmetric about the two principal directions. As expected from theory, this particular network of continuous fractures has the same flow behavior as a porous medium.

Having demonstrated that this system of continuous fractures behaves like a porous medium for fluid flow, the model was next used to investigate equivalent porous medium behavior for transport. For comparison, one needs the total porosity of the fracture system. The porosity of each set is 0.0002, which is simply the 0.002-cm aperture divided by the 10-cm spacing, and therefore the total porosity for the two sets is 0.0004.

Figure 10 is a plot of the hydraulic effective porosity versus direction of flow, which was determined by adding the angle of flow to the orientation of the flow region. At orientation 90° (where the numerical flow direction is 90 − 61.3 = 28.7°) and orientation 120° (where the numerical flow direction is 181.3°) there is a dramatic reduction in ϕ_H. At either orientation, one set of fractures becomes nonconductive because it is perpendicular to the hydraulic gradient. The result is that ϕ_H is equal to $\phi/2$ in either flow direction. The directional dependence in the hydraulic effective porosity shows that this fracture system does not behave as an equivalent porous medium for transport.

At orientation 105°, ϕ_H decreases slightly below ϕ and obtains a value of 0.000384. To check this result, two additional square flow regions of widths 320 and 450 cm were tested at this same orientation. The resulting ϕ_H were 0.000385 and 0.000409, respectively. This indicates that the original result was a scale effect, because as the flow region size increased, ϕ_H converged to ϕ. However, the rate of this convergence is seen to be a function of flow direction.

The change in convergence rate is directly related to the tortuosity τ, which is the ratio of the mean path length to the linear travel length. As tortuosity increases, travel paths become more irregular because the paths deviate more from the direction of flow. Consequently, larger flow regions are needed before representative mechanical transport behavior occurs. Figure 11 shows that the tortuosity is approximately 1.04 between directions 0° to 30°. Near direction 30°, the tortuosity reaches a minimum of 1.0 because fluid flows in only one of the sets. The tortuosity then increases rapidly to 3.86 at flow direction 105°. The bisection of the hydraulic gradient, with the obtuse angle of 150° resulting from the intersection of the two fracture sets, caused tortuosity to be maximum in this direction. Thus the large tortuosity in this direction results in a slight oscillation in ϕ_H.

The mean pore velocity MPV is defined as

$$\text{MPV} = \frac{1}{V_c}\int_{V_c} u\, dV_c$$

The mean pore velocity is normally difficult to compute because the velocity in each pore (element) must be known. Consequently, an estimate of mean pore velocity, VPORE,

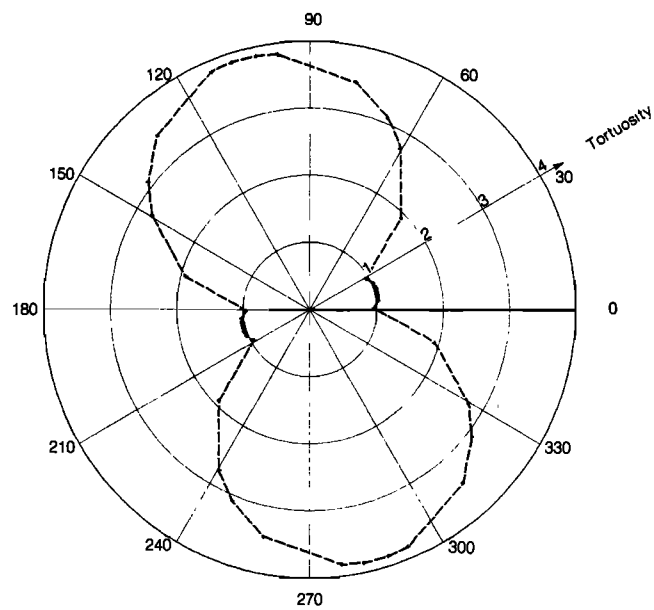

Fig. 11. Polar plot of tortuosity for system with two sets of parallel, continuous, and constant aperture fractures.

was developed in this study by using two macroscopic mechanical transport parameters that are easier to measure than the individual microscopic pore velocities:

$$\text{VPORE} = (\text{VLIN})\tau$$

This expression was determined by substituting VLIN for q/ϕ into the derivation of the Kozeny equation [*Wyllie and Spangler*, 1952].

Figure 12 shows a plot of VPORE versus the direction of flow. This figure shows the VPORE is an excellent estimator of mean pore velocity provided that the correct directional values of τ are used. In transport studies, tortuosity is rarely known and normally assigned a value about $\sqrt{2}$. Figure 12 also demonstrates that if a constant tortuosity of $\sqrt{2}$ had been used to compute VPORE, an error in the mean pore velocity would have resulted.

If the hydraulic effective porosity is a constant, then the square root of the average linear velocity divided by cos θ, $(\text{VLIN}/\cos\theta)^{1/2}$, should plot as an ellipse for an equivalent porous medium, since $(q/\cos\theta)^{1/2}$ would plot as an ellipse. The plot of $(\text{VLIN}/\cos\theta)^{1/2}$ in Figure 9*b* also demonstrates that this fracture system cannot be treated like an equivalent porous medium. Although the VLIN curve coincides with the q curve in most directions, there are four sharp cusps in the directions where ϕ_H drops dramatically.

System with Two Orthogonal Sets of Fractures

In the second investigation with this model the system consisted of two orthogonal sets of parallel fractures. All fractures of the same set were spaced 10 cm apart. Anisotropy was achieved by using an aperture of 0.002 cm for the first set oriented at 0° and an aperture of 0.004 cm for the second set oriented at 90°. Thus the direction of maximum principal permeability is 90°, and the direction of minimum principal permeability is 0°. The hydraulic gradient along sides 1 and 3 (see Figure 5) was set at 0.01 for all flow regions. The total porosity is 0.0006; the porosity for the set oriented at 0° is 0.0002, and that for the set at 90° is 0.0004.

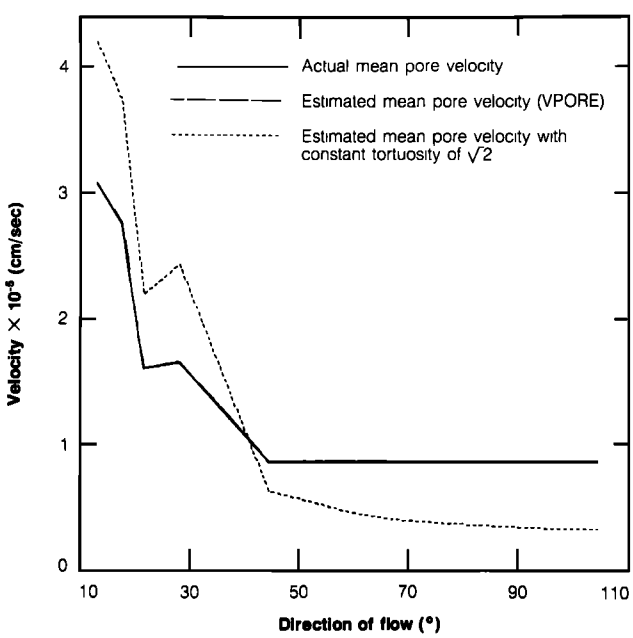

Fig. 12. Actual mean pore velocity, estimated mean pore velocity, and estimated mean pore velocity with constant tortuosity of $\sqrt{2}$.

TABLE 2. Specific Discharge Results for Fracture System With Two Orthogonal Sets of Fractures

Orientation of Gradient, degrees	Specific Discharge, 10^{-7} cm/s		Angle of Flow, degrees		
	Theoretical	Numerical	Theoretical	ANFC	ANFD
0	0.6538	0.6538	0	−0.31	−0.40
15	1.496	1.499	49.99	50.91	50.90
30	2.676	2.691	47.78	47.52	46.82
45	3.727	3.681	37.87	38.08	37.87
60	4.541	4.668	25.87	25.64	25.12
75	5.055	5.086	13.08	14.72	14.59
90	5.230	5.230	0	0	0

Sizes of flow regions were selected so that the number of elements and nodes in each region was nearly equal to that of the first study. It was anticipated that using the same number of elements and nodes would produce equivalent porous medium flow behavior in this orthogonal fracture system. Square flow regions of width 280 cm were used for orientations 0°, 45°, 60°, 75°, and 90°. Rectangular flow regions of 235 × 335 cm were used for orientations 15° and 30° because the angle of flow was greater than 45°

A comparison of numerical and theoretical values for specific discharge is given in Table 2. The results demonstrate that each flow region behaves like an equivalent porous medium for fluid flux. Figure 13*a* is further evidence that this system of orthogonal fractures behaves like an equivalent porous medium for fluid flux. The plot of $(q/\cos\theta)^{1/2}$ is an ellipse whose maximum axis coincides with the direction of the maximum permeability at 90° and whose minimum axis coincides with the direction of the minimum permeability at 0°.

The model was next used to investigate continuum behavior for transport, and the results are shown on Figure 14. We again see a drastic reduction in hydraulic effective porosity when the direction of gradient is at right angles to either fracture set. Figure 14 clearly illustrates the directional dependence of hydraulic effective porosity for this orthogonal fracture system. The plot of $(\text{VLIN}/\cos\theta)^{1/2}$ in Figure 13*b* reveals an unexpected result. One would normally associate the direction of minimum permeability as an indication of the direction for the minimum linear velocity. However, the minimum value of VLIN does not occur at 0° because the minimum hydraulic effective porosity occurs in this direction. In dealing with fracture networks of this kind, one simply cannot associate directions of principal permeabilities with the directions of maximum and minimum linear velocities.

CONCLUSIONS AND RECOMMENDATIONS

The objectives of this paper were to investigate directional mechanical transport properties for anisotropic fracture systems, to determine when fracture systems can be treated like equivalent porous media in transport studies, and to introduce a model that simulates mechanical transport in networks of fractures. The two important conditions necessary for measuring directional mechanical transport for an equivalent porous medium are a uniform flow field and a test section where the linear path length is constant. When these two conditions are satisfied, mechanical transport parameters can be measured from the breakthrough curve for the fluid that flows within the test section.

The hydraulic effective porosity was defined as the ratio of specific discharge to average linear velocity. In porous media

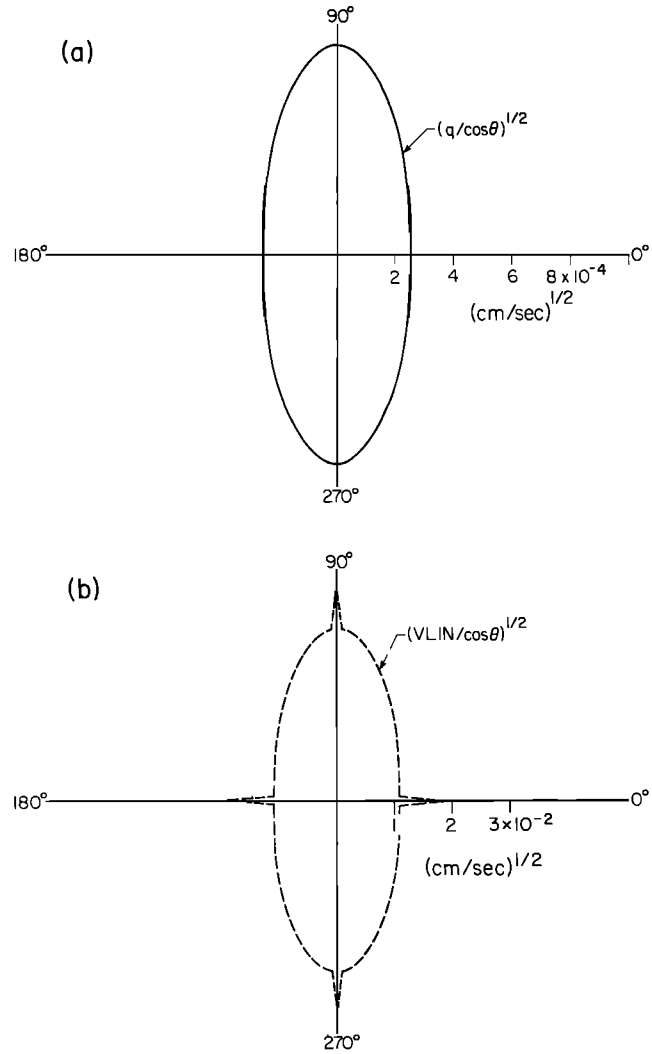

Fig. 13. Polar plots of (*a*) specific discharge and (*b*) average linear velocity factors versus direction of flow for system with two orthogonal sets of fractures.

transport studies, hydraulic effective porosity is directionally stable. Thus the shape of the polar plot of hydraulic effective porosity was used to test whether a fracture system behaved like an equivalent porous medium for transport.

A numerical model was developed to simulate mechanical transport under steady flow in a network of fractures. The model incorporated the principles of laminar flow to calculate the location of streamtubes for fluid flowing from one side of a flow region to another. The model has been used to simulate mechanical transport in regular, anisotropic systems of continuous fractures.

The results demonstrated that a fracture system which behaves as a continuum for fluid flux may not behave as a continuum for mechanical transport. This was demonstrated by a case in which hydraulic effective porosity was directionally dependent and decreased well below the total porosity in certain directions. In these directions a fracture set became nonconductive because the direction of the hydraulic gradient was perpendicular to the orientation of the set. In other directions the hydraulic effective porosity was equal to the total porosity. An important effect of this decrease in hydraulic effective porosity was that the directions of maximum and minimum linear fluid velocities did not necessarily coincide with the directions of the principal permeabilities.

The size of the flow region required for mechanical transport continuum behavior was found to be related to tortuosity. As tortuosity increased, travel paths became more irregular and deviated more from the mean direction of flow. Consequently, when tortuosity was large, larger flow regions were needed before representative mechanical transport behavior occurred. VPORE, computed as the product of tortuosity and average linear velocity, was shown to be a good estimate of the mean pore velocity.

Application of this numerical model to more realistic fracture systems is needed. A dramatic drop in hydraulic effective porosity is unlikely to occur in random fracture systems because the irregular nature of the interconnected flow paths will inhibit abrupt changes in the conductive nature of the overall network. The void spaces in a system of discontinuous fractures form a complex network of conductive fracture segments, dead-end spaces, and isolated zones where no communication with the general network exists. Studies using stochastically generated discontinuous networks are presently being conducted to investigate the factors that affect mechanical transport through such fracture systems. The work is also investigating the dependence of longitudinal mechanical dispersion on the direction of flow.

Acknowledgments. This work was funded by the U.S. Department of Energy under contract DE-AC-03-76SF00098.

NOTATION

ANFC angle of flow based on uniformity of flow, degrees.
ANFD angle of flow based on components of specific discharge, degrees.
b fracture aperture, cm.
c concentration, g/cm^3.
c_0 concentration in an outflow fracture, g/cm^3.
g acceleration of gravity, cm/s^2.
L linear length of travel, cm.
L_c width on side 2 of zone of continuous flow from side 2 to 4, cm.
L_{NC} width on side 2 of zone of noncontinuous flow from side 2 to 4, cm.
L_T length of element, cm.
L_x width of flow region, cm.
L_y height of flow region, cm.

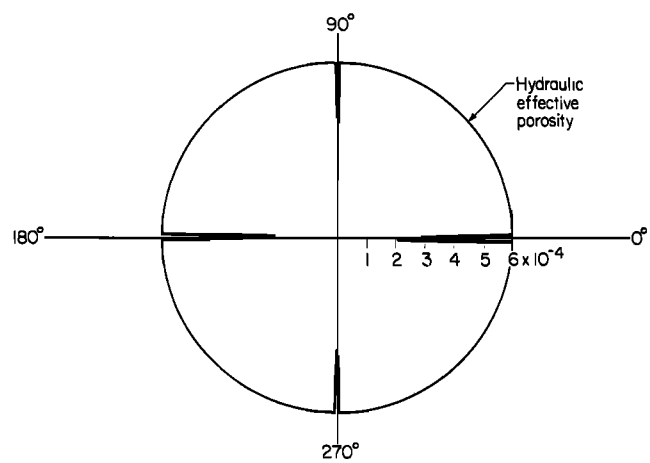

Fig. 14. Polar plot of hydraulic effective porosity versus direction of flow for system with two orthogonal sets of fractures.

MPV actual mean pore velocity, cm/s.
$\mathbf{q}$ specific discharge, cm/s.
q_T theoretical magnitude of specific discharge, cm/s.
Q_C continuous flow rate from side 2 to 4, cm^2/s.
Q_f flow rate in element, cm^2/s.
Q_N total flow rate into node, cm^2/s.
Q_{NC} flow rate into side 2 that does not exit on side 4, cm^2/s.
Q_{ST} flow rate in stream tube, cm^2/s.
Q_x flow rate in x direction of flow, cm^2/s.
Q_{S1} flow rate into side 1, cm^2/s.
Q_{S2} flow rate into side 2, cm^2/s.
Q_{S3} flow rate out of side 3, cm^2/s.
Q_{S4} flow rate out of side 4, cm^2/s.
t time, s.
t_{ST} travel time of fluid in stream tube in element, s.
u fracture velocity, cm/s.
V_c void volume, cm^3.
VLIN average linear velocity, cm/s.
VPORE calculated estimate of mean pore velocity, cm/s.
η ordinate of coordinate system inside fracture, cm.
θ angle of flow, degrees.
θ_T theoretical angle of flow, degrees.
μ fluid viscosity, dynes- s/cm^2.
ξ abscissa of coordinate system inside fracture, cm.
ρ fluid density, g/cm^3.
τ tortuosity.
ϕ total porosity.
ϕ_H hydraulic effective porosity.
ϕ_T theoretical porosity.
Φ hydraulic head, cm.

REFERENCES

Biggar, J. W., and D. R. Nielsen, Diffusion effects in miscible displacements occurring in saturated and unsaturated porous materials, *J. Geophys. Res.*, *65*(9), 2887–1895, 1960.

Castillo, E., R. J. Krizek, and G. M. Karadi, Comparison of dispersion characteristics in fissured rocks, *Proc. Symp. Fundam. Transp. Phenom. Porous Media 2nd*, 778–797, 1972.

Freeze, R. A., and J. A. Cherry, *Groundwater*, 604 pp., Prentice-Hall, New York, 1979.

Grove, D. B., and W. A. Beetem, Proosity and dispersion constant calculations for a fractured carbonate aquifer using the two-well tracer method, *Water Resour. Res.*, *7*(1), 128–134, 1971.

Hazzaa, I. B., K. F. Saad, R. K. Girgis, A. A. Bakr, and F. M. Swailem, Determination of porosity of groundwater aquifers by the radioactive tracer technique, *Int. J. Appl. Radiat. Isot.*, *16*, 261–265, 1965.

Hazzaa, I. B., R. K. Girgis, K. F. Saad, F. M. Swailem, and A. A. Bakr, Study of the applicability of different radioisotopes for determination of the porosity of groundwater aquifers, *Int. J. Appl. Radiat. Isot.*, *17*, 621–628, 1966.

Hoehn, E., and P. V. Roberts, Advection-dispersion interpretation of tracer observations in an aquifer, *Groundwater*, *20*(4), 457–465, 1982.

Karadi, G. M., R. J. Krizek, and E. Castillo, Hydrodynamic dispersion in a single rock joint, *J. Appl. Phys.*, *43*(12), 5013–5021, 1972.

Krizek, R. J., G. M. Karadi, and E. Socias, Mathematical model for two-dimensional percolation through fissured rock, paper presented at the Symposium on Percolation Through Fissured Rock, Int. Soc. for Rock Mech., Stutgart, 1972.

Long, J. C. S., J. S. Remer, C. R. Wilson, and P. A. Witherspoon, Porous media equivalents for network of discontinuous fractures, *Water Resour. Res.*, *18*(3), 645–658, 1982.

Marcus, H., and D. E. Evenson, Directional permeability in anisotropic porous media, *Water Resour. Ctr. Contrib. 31*, 105 pp., University of California, Berkeley, 1961.

Schwartz, F. W., L. Smith, and A. S. Crowe, Stochastic analysis of groundwater flow and contaminant transport in a fractured rock system, paper presented at the Symposium on the Scientific Basis of Nuclear Waste Management, Mater. Res. Soc., Boston, 1981.

Snow, D. T. Anisotropic permeability of fractured media, *Water Resour. Res.*, *5*(6), 1273–1289, 1969.

Von Rosenburg, D. U., Mechanics of steady state single-phase fluid displacement from porous media, *AIChE J.*, *2*(1), 55–58, 1956.

Wilson, C. R., An investigation of laminar flow in fractured porous rocks, Ph.D. thesis, 178 pp., Univ. of Calif., Berkeley, 1970.

Wyllie, M. R. J., and M. B. Spangler, Application of electrical resistivity measurements to problem of fluid flow in porous media, *Bull. Am. Assoc. Pet. Geol. 36*(2), 359–403, 1952.

H. K. Endo, J. C. S. Long, and P. A. Witherspoon, Earth Science Division, Lawrence Berkeley Laboratory, 1 Cyclotron Road, Berkeley, CA 94720.

C. R. Wilson, Hydrotechnique Associates, 661 Vistamont Avenue, Berkeley, CA 94708.

(Received August 23, 1983;
revised May 7, 1984;
accepted May 31, 1984.)